CONVECTIVE HEAT AND MOISTURE TRANSPORT IN A PARTIAL ENCLOSURE WITH MULTIPLE PORTS AND MULTIPLE FLOWS

Fu-Yun Zhao* **Sanjeeva Witharana** **Joyleen Poole** **Yu-Long Ding**

School of Process, Environmental and Materials Engineering
Faculty of Engineering, University of Leeds
Houldsworth Building, Leeds, LS2 9JT, England, UK

*Email – F.Y.Zhao@leeds.ac.uk

ABSTRACT

Simultaneous transport of heat and moisture by natural convection in a partial enclosure with four free ports is investigated numerically. Moist air motions are driven by the temperature and concentration differences resulting from ambient air and internal discrete sources, with different levels of temperature and concentration. The Prandtl number and Schmidt number used are 0.7 and 0.6 respectively. Due to boundary conditions and geometries are symmetric about vertical mid-plane, only half space is taken into consideration by use of symmetrical boundary conditions. The fluid, heat and moisture transports through the cavity are respectively analyzed using the streamlines, heatlines and masslines, and the heat and mass transfer potentials are also explained by the variations of overall Nusselt and Sherwood numbers. The numerical simulations presented here span a wide range of the thermal/solutal levels of external and internal sources in the domain of aiding buoyancy forced flows. Multiple steady flows appear as different initial distributions were imposed. It is shown that the heat transfer potential, moisture transfer potential, and flow patterns can be promoted or inhibited, depending strongly on the thermal/moisture Rayleigh numbers and initial flow states.

INTRODUCTION

Natural convection in enclosures has received extensive attentions because it is vital in understanding many aspects of buoyancy driven flows and also it has various engineering applications. Among these, natural convection in enclosures with open sides or natural-vented openings has received relatively few attentions probably due to the complexity of computations with the open sides. Buoyancy driven flows in open cavities actually occur in many fields, for instance, solar energy collector, nuclear waste repository, thermosiphons, cooling of electrical components, building ventilation, to name just a few (Gebhart et al. 1988). Several authors have experimentally and theoretically studied natural convection in an open or partial cavity, considering the effects of geometries, internal separation, aperture size and location, inclination angle relative to gravitation, fluid properties, thermal boundary conditions, transient state, and momentum conditions at the open sides, also mixing with other heat transfer processes, radiation heat transfer or conjugate heat transfer (Chan and Tien 1985a, Chan and Tien 1985b, Abib and Jaluria 1988, Angirasa 1992, Desrayaud and Lauriat 2004, Lal and Reji 2009).

Aforementioned studies deal with fluid motion due only to temperature gradients, i.e., single-component natural convection. Nevertheless, fluid motion may be induced by density variations due to gradients of other scalar quantities. One of these quantities can be pollutant concentration within the fluid. Such a phenomenon, combining temperature and concentration buoyancy forces, is called multi-component flow or double diffusion (Ingham and Pop 2005). Taking essentially the building construction elements as an example, the convection motion of moist air results from the different levels of temperature and moisture concentration, thus giving rise to a double diffusive free convective fluid flow. Similar situations could be found in electronics with passive heating and contaminant infiltration, hazardous thermo-chemical spreading, solar pond and liquid fuel storage, grain storage, food processing and storage, to name just a few. Relative to a large volume of published studies on this phenomenon in pure fluids, the thermosolutal convection in enclosures, particularly the combined heat and moisture convective transport, has received only limited attention (Beghein et al. 1992, Costa 1997, Chamkha and Al-Naser 2002, Liu et al. 2008, Zhao et al. 2007, Zhao et al. 2008).

In the present work, double diffusive natural convection occurring in the partial enclosure with four free vented ports is investigated. At the same time, the ambient moist air is of high temperature and high relative humidity, just modeling the summer days in most regions across the world. Particularly, the ensued fluid flow undergoes multiple steady flow patterns as different initial distributions are imposed (Zhao et al. 2008). Additionally, visualization of the heat and moisture convective transports, using streamlines, heatlines and masslines (Beghein et al. 1992, Costa 1997, Liu et al. 2008, Zhao et al. 2007, Zhao et al. 2008), would be conducted, such that the transport paths of fluid, heat and moisture in the fluid cavity and walls would be presented clearly and vividly.

Problems relevant to oscillatory or subcritical solutions are not analyzed; the corresponding combinations of the dimensionless governing parameters and boundary conditions leading to such phenomena are intentionally avoided. In the following sections, physical model of an enclosure with four free-vent openings is first presented. Next, the mathematical formulation is delineated and numerical methods are validated by benchmark solutions. With that, combined heat and moisture transfer in the enclosure is examined for different thermal and concentration buoyancy parameters.

PHYSICAL AND MATHEMATICAL STATEMENTS

The domain under analysis is sketched in Fig. 1, where a rectangular enclosure is filled with a fluid containing a pollutant concentration whose mass transfer occurs is under the influence of the gravity field. The

third-dimension of the domain is assumed to be large so that a two-dimensional analysis can be applied. The gravitational acceleration acts in the negative y-direction, vector (u, v) parallels to coordinate (x, y) accordingly. As seen at the continuum visual resolution, the rectangular enclosure of $W \times H$ is bounded with four free openings respectively located top right of height d_{RU}, bottom right of height d_{RL}, top left of height d_{LU} and bottom left of height d_{LL}. A thermosolutal source is centrally located on the bottom wall, being of d_i.

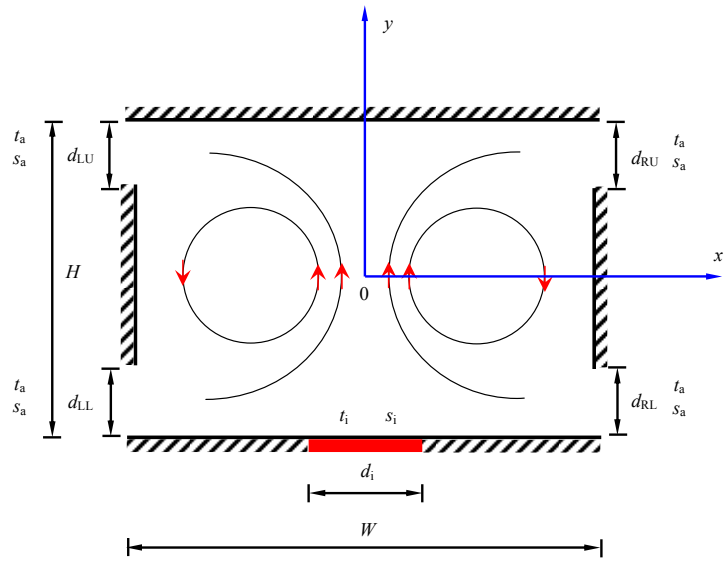

Figure 1 - Physical model and Cartesian coordinates of the present study

Model assumptions

Horizontal walls excluding the thermoslutal source and vertical sides excluding free ports are assumed to be impermeable and perfect thermal insulations. The surroundings of the enclosure is maintained at constant and uniform different levels of temperature and concentration (t_a and s_a), while the internal source surface maintains constant temperature t_i and concentration s_i. As stated before, summer climate conditions can be represented by the following relations, $t_a > t_i$, and $s_a > s_i$, typically as warm and humid ambient climate.

Accordingly, temperature and concentration gradients are imposed on the fluid, and the flow is then initiated and evolves under the action of the combined or aided driving forces due to these gradients. Air, heat and moisture from the indoor and outdoor are transferred by natural convection to/from a fluid circulating through the openings to a fluid reservoir at different levels of temperature and concentration.

The double diffusion model considered here assumes steady laminar flow, both components (air and contaminant) in the gaseous mixture to be perfectly mixable, and the Soret, Dufour and species inter-diffusion effects are negligible. All the physical properties are supposed to be independent of the temperature and concentration, except the mixture density variations in the vertical momentum source term, for which the Boussinesq approximation is used, i.e., $\rho = \rho_r[1 - \beta_t(t - t_r) - \beta_s(s - s_r)]$, where reference temperature t_r and concentration s_r are respectively determined by $(t_a+t_i)/2$ and $(s_a+s_i)/2$; β_t is the volumetric thermal expansion coefficient and, similarity, β_s is the volumetric mass expansion coefficient relative to concentration. It is worth noting that the concentration expansion coefficient is slightly different from the thermal one, β_t (air) is always positive (an increase in temperature induces a decrease in density) while β_s may be either positive or negative (an increase in pollutant concentration, respectively, induces a decrease or an increase in density). Additionally, all the heat and mass transfer properties of the involved media (two mixture components, the mixture and the solid

wall) are assumed to be constant, except for the density appearing in the buoyancy terms, as explained foregoing.

Model equations

Recognizing that convection and diffusion terms must maintain balance and considering the ranges of governing parameters in the present work, H, U_0 $[(g\beta_t\triangle tH)^{1/2}]$, $\triangle t$ (t_a-t_i) and $\triangle s$ (s_a-s_i) are introduced as characteristic scales for length, velocity, temperature and concentration respectively (Zhao et al. 2006). Basing on the aforementioned assumptions and characteristic scales, the set of equations that describe the conservations of continuity, momentum, energy and concentration transports can be expressed in dimensionless form as follows,

$$\frac{\partial U}{\partial X}+\frac{\partial V}{\partial Y}=0 \tag{1}$$

$$\frac{\partial UU}{\partial X}+\frac{\partial VU}{\partial Y}=-\frac{\partial P}{\partial X}+\sqrt{\frac{\mathrm{Pr}}{Ra}}\left(\frac{\partial^2 U}{\partial X^2}+\frac{\partial^2 U}{\partial Y^2}\right) \tag{2}$$

$$\frac{\partial UV}{\partial X}+\frac{\partial VV}{\partial Y}=-\frac{\partial P}{\partial Y}+\sqrt{\frac{\mathrm{Pr}}{Ra}}\left(\frac{\partial^2 V}{\partial X^2}+\frac{\partial^2 V}{\partial Y^2}\right)+(T+NS) \tag{3}$$

$$\frac{\partial UT}{\partial X}+\frac{\partial VT}{\partial Y}=\frac{1}{\sqrt{Ra\,\mathrm{Pr}}}\left(\frac{\partial^2 T}{\partial X^2}+\frac{\partial^2 T}{\partial Y^2}\right) \tag{4}$$

$$\frac{\partial US}{\partial X}+\frac{\partial VS}{\partial Y}=\frac{1}{Le\sqrt{Ra\,\mathrm{Pr}}}\left(\frac{\partial^2 S}{\partial X^2}+\frac{\partial^2 S}{\partial Y^2}\right) \tag{5}$$

Above equations were non-dimensionalized by introducing the following definitions,

$$(X,Y)=(x,y)/H,\ (U,V)=(u,v)/U_0,\ P=(p+\rho_r gy)/[\rho_r U_0^2],\ T=(t-t_r)/\triangle t,\ S=(s-s_r)/\triangle s \tag{6}$$

Foregoing equations are emerging the dimensionless parameters,

$$Pr=\nu/\alpha,\ Ra=g\beta_t\triangle tH^3/\nu\alpha,\ Le=\alpha/D,\ N=\beta_s\triangle s/\beta_t\triangle t \tag{7}$$

Where, Le represents the ratio between the thermal and compositional diffusivities. For liquid solutions, thermal diffusivity is considerably higher than mass diffusivity, and this is one of the causes of many remarkable patterns of these flows, like convective cells separated by sharp interfaces (Ingham and Pop 2005). For air mixtures, however, Beghein et al. (1992) pointed out that the Lewis numbers of different kinds of pollutants mixed with air might vary between 0.2 and 5 (25 ℃ and 1 atm). When equations (4) and (5) have the same boundary conditions, the T and S fields are coincident if Le equaling unity.

Boundary conditions

Non-slip boundary conditions are imposed over the solid wall and solid boundaries of the enclosure. With such boundary conditions, it is assumed that the pollutant mass flow through the horizontal walls is small enough in order to validate the use of zero normal velocity values at such walls. Prescription of T and S over the surface of strip source in the center floor and those of ambient environment can be stated as follows,

$$T = -0.5,\ S = -0.5 \qquad -d_i/2H \le X \le +d_i/2H,\ Y = -1/2 \tag{8}$$

$$T = +0.5,\ S = +0.5 \qquad -d_i/2H >> X \text{ or } +d_i/2H << X \tag{9}$$

With regard to the numerical domain that is restricted to the cavity fluid, the planes along the openings separate the cavity from the fluid reservoir. The energy and species conditions imposed at the openings are the same as those used by Chan and Tien (1985b), that is to say, the fluid that enters the cavity has the same temperature and concentration as the reservoir, while the boundary regions through which the fluid leaves the cavity satisfy the upwind conditions. Mathematically, these could be expressed as,

$$\text{At the entrance port } (U_{X=-W/2H} > 0 \text{ or } U_{X=W/2H} < 0),\ T = 0.5,\ S = 0.5 \tag{10}$$

$$\text{At the exit port } (U_{X=-W/2H} < 0 \text{ or } U_{X=W/2H} > 0),\ \partial T/\partial n = 0,\ \ \partial S/\partial n = 0 \tag{11}$$

This condition is based on the assumption that in the boundary layer flow that crosses the openings the contribution due to the longitudinal convection is much greater than the contribution due to lateral/tangential convection. This is particularly valid at moderate and high Rayleigh numbers, which is in the flow region with distinct boundary layers.

For the momentum boundary conditions, the derivative of tangential velocity is set at zero, while the longitudinal component of velocity on the openings is obtained by the mass balance at the boundary cells. The mass conservation across this enclosure has been got around by the efficient solution of pressure correction equations. The simulated results have been compared with those of extended domain method, which demonstrates that the present boundary assumptions are valid, particularly as opening sizes are less than 1/2 and thermal Rayleigh number exceeds 10^4. Detailed numerical comparisons with benchmark results will also be presented in the following sections.

Convective transport and visualization

Overall Nusselt number and Sherwood number along the sink surface on the floor Nu and Sh are obtained respectively as,

$$Nu = \int_{-d_i/2}^{d_i/2} -\left.\frac{\partial T}{\partial Y}\right|_{Y=-1/2} dX,\ \ sh = \int_{-d_i/2}^{d_i/2} -\left.\frac{\partial S}{\partial Y}\right|_{Y=-1/2} dX \tag{12}$$

In order to clearly exhibit the fluid, heat and contaminant transport characteristics of double-diffusive natural convection, a recently developed visualization technique of convective transport paths is employed (Costa 1997,

Zhao et al. 2007). In terms of above continuity, energy, and concentration conservation equations in the fluid domain, the dimensionless streamfunction Ψ, heatfunction Θ, and massfunction Ω are defined respectively as follows,

$$\frac{\partial \Psi}{\partial Y} = U\,, \quad -\frac{\partial \Psi}{\partial X} = V \tag{13}$$

$$\frac{\partial \Theta}{\partial Y} = \sqrt{Ra\,\mathrm{Pr}}UT - \frac{\partial T}{\partial X}\,, \quad -\frac{\partial \Theta}{\partial X} = \sqrt{Ra\,\mathrm{Pr}}VT - \frac{\partial T}{\partial Y} \tag{14}$$

$$\frac{\partial \Omega}{\partial Y} = Le\sqrt{Ra\,\mathrm{Pr}}US - \frac{\partial S}{\partial X}\,, \quad -\frac{\partial \Omega}{\partial X} = Le\sqrt{Ra\,\mathrm{Pr}}VS - \frac{\partial S}{\partial Y} \tag{15}$$

The corresponding contour lines, streamlines, heatlines and masslines, are representatives of the transport pathlines of fluid, heat and contaminant (Zhao et al. 2007).

NUMERICAL METHODS

Since the flow governed by equations (1)-(5) is known to be elliptic in space, iterative procedures must be employed to obtain the solution in the spatial domain. Finite volume method (FVM) is applied to discretize the governing equations on a staggered grid system (Patankar 1980). In the course of discretization, the third-order deferred correction QUICK scheme (Hayase et al. 1992) and a second order central difference scheme are respectively implemented for the convection and diffusion terms. The SIMPLE algorithm was chosen to numerically solve the governing differential equations in their primitive form (Patankar 1980). The pressure correction equation is derived from the continuity equation to enforce the local mass balance (Patankar 1980).

The discretized equations were solved by a line-by-line procedure, combining the tri-diagonal matrix algorithm (TDMA) and the successive over-relaxation (SOR) iteration. These equations were alternatively swept in the X and Y directions until the relative changes between two consecutive iterations in all dependent variables (U, V, T and S) at every nodal point were below 10^{-5}. The solutions for the pressure correction equation were iterated until the local mass balance was achieved to a satisfactory degree. Steady state was considered to be attained by two criteria. First of all, the solutions at every node should become almost unchanged with time. Additionally, reliable numerical results were obtained by performing energy and mass balances over the physical domain (Zhao et al. 2006, Zhao et al. 2009).

RESULTS AND DISCUSSION

Absolutely, the coupled heat and mass transfer in this enclosure is affected by lots of parameters. As rudimental studies, the geometries are fixed, i.e., $W = 2H$, $d_{RU} = d_{RL} = d_{LU} = d_{LL} = H/10$. The size of floor sink maintains at $d_i = W/5$. Due to the symmetries of geometry and boundary conditions imposed on this system shown in Fig.1, a symmetrical boundary conditions are imposed along the vertical mid-plane X=0. Thus, only half of the flow fields are illustrated in following results.

Basic flow situations

Firstly, moist air is composed of moisture and air, its Prandtl and Schmidt numbers can be determined for room temperature and normal ambient air bar. Usually, Pr = 0.7, Le = 0.8 are maintained across this study. Thermal Rayleigh number Ra is maintained at 10^5 for temperature difference between indoor and surroundings being less than 5℃. Depending on the buoyancy ratio, the double diffusion can undergo thermal driven natural convection (N = 0), solutal-dominated convection (N>>1) and intermittent convection with suitable buoyancy ratios. As illustrated in Fig. 2, the results of steady flows are obtained respectively for thermal-driven natural convection and solutal dominated convection.

As the thermal buoyancy force solely acts on the fluid flow, two symmetric weak large flow circulation respectively consisting of two secondary eddies presents in Fig. 2(a) of N = 0. As a consequence, both the isotherms and iso-concentrations tend to be diffusive distributed across the enclosure, just like the thermal and solutal stratifications, temperature and concentration of air mixture in upper space are higher than those in the lower space. Observing from the heatlines and masslines shown in Fig. 2(a), heat and moisture transports from ambient to the floor sink, flowing into the upper vents and vertically across the space and into the floor sink.

As buoyancy ratio increases up to 5, as shown in Fig. 2(b) of N = 5, solutal buoyancy force greatly exceeds that thermal one, air flow impelled by the aiding effect of both forces occurs at both lower left and lower right corners, and then bifurcates, one forms two symmetric large flow circulations occupying most space of the enclosure, while the other directly transports to the upper openings. Correspondingly, heat and moisture are transported from the ambient via lower vents, one being directly exhausted to the surroundings via upper vents, while the other being circulated into the floor sink. Additionally, heat and moisture are uniformly distributed across most space of the enclosure, great thermal and solutal gradients clustering around the lower vents and floor sink.

Multiple steady flow situations

Aforementioned flow charts are all obtained using the rest state ($\Psi = T = S = 0$) as initial conditions. However, multiple steady solutions are possible when different initial conditions are used. An example of this flow configuration is given in Fig. 3 with N = 2. Figs. 3(a) and 3(b) are obtained respectively using the flow fields illustrated in Fig. 2(a) and Fig. 2(b) as initial conditions. Interestingly, heat and moisture transports shown in Fig. 3(a) almost are of dominantly diffusive mode, which is similar to that of N = 0 illustrated in Fig. 2(a); whereas, that flow patterns and heat/mass transports in Fig. 3(b) tend to be similar to those shown in Fig. 2(b). Although the boundary conditions are completely same, the flow charts and heat/moisture transport routes are completely different. This multiple flow phenomena can be employed for actual engineering applications.

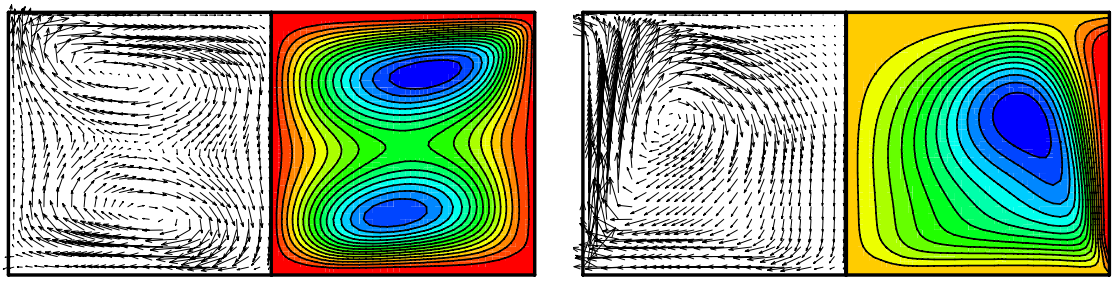

Vectors and streamlines

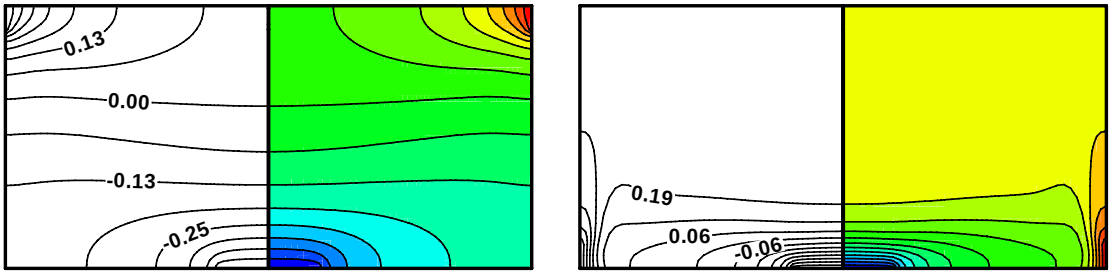

Isotherms

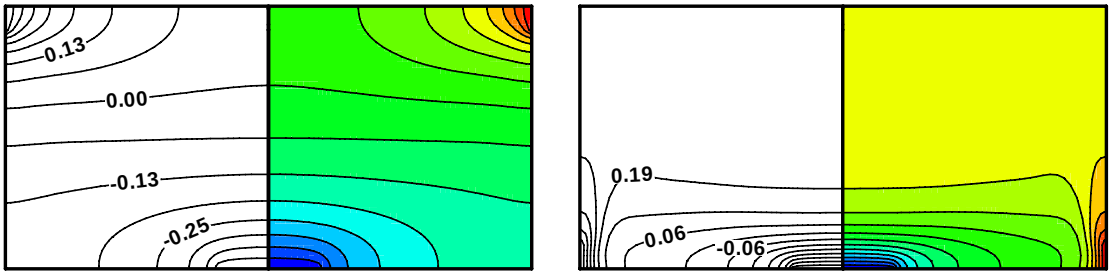

Iso-concentrations

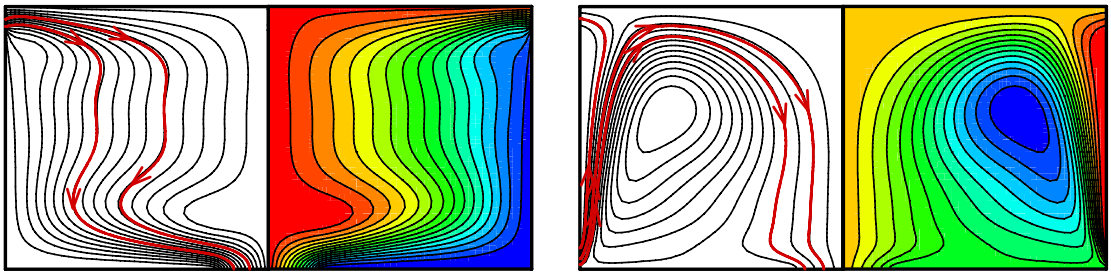

Heatlines

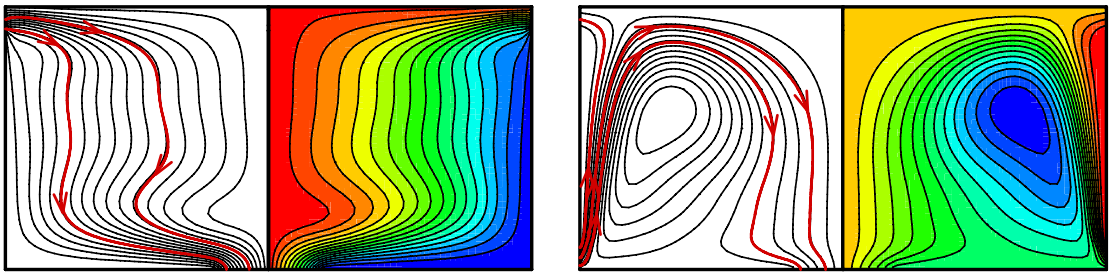

Masslines

(a) $N = 0$ (b) $N = 5$

Figure 2 Steady flow results of thermal driven natural convection (N=0) and solutal-dominated convection (N=5)

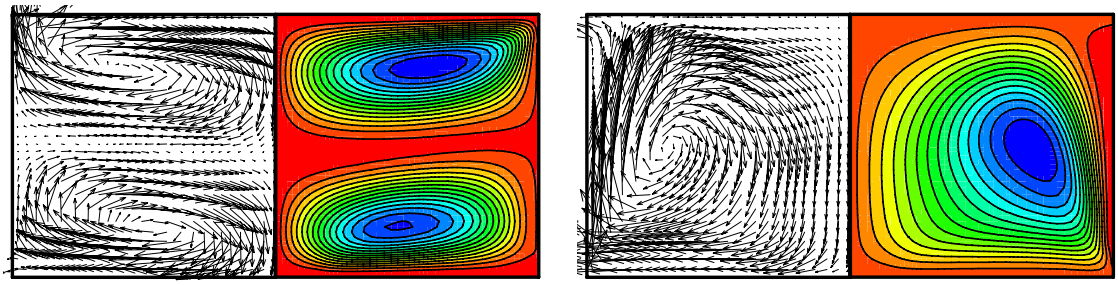

Vectors and streamlines

Isotherms

Iso-concentrations

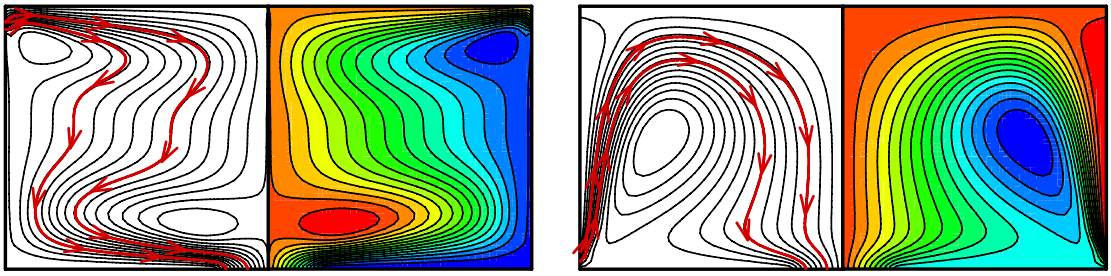

Heatlines

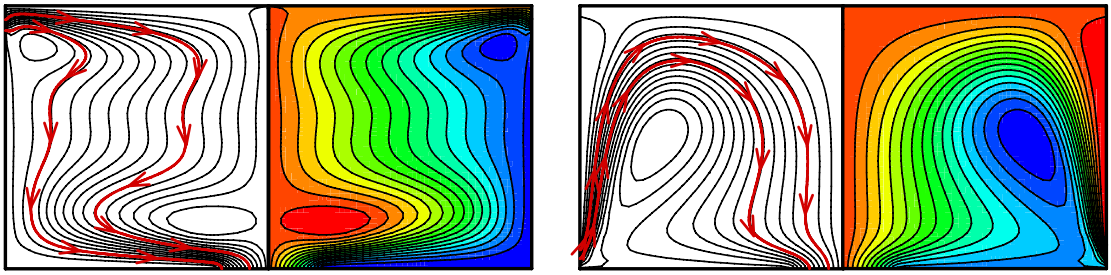

Masslines

(a) $N = 2$ (b) $N = 2$

Figure 3 - Multiple steady flow results of double diffusive natural convection (N=2)

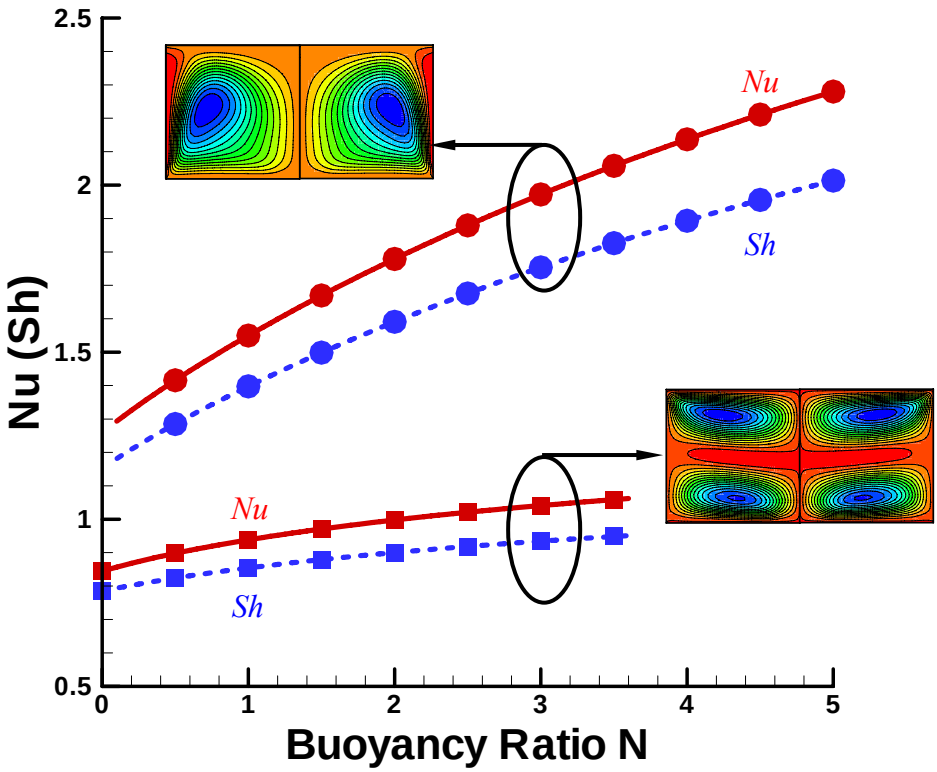

Figure 4 – Heat and mass transfer rates along the floor sink surface.

Convective transfer rates

The effect of buoyancy ratio N on the overall Nusselt and Sherwood numbers is depicted in Fig. 4 for $Ra = 10^5$, $Le = 0.8$ and $0 \leq N \leq +5$. In general, heat and mass transfer rates increase with increasing buoyancy ratios. Here should be noted that the moisture boundary layer is thicker than that of thermal boundary layer due to Lewis number is less than unity. As a consequence, convective mass transfer rate (*Sh*) is lower than that heat transfer rate *Nu*.

For the convection-dominated solutions, using the flow patterns of Fig. 2(b) and $N = 5$ as initial distributions, gradually decreasing buoyancy ratios from $N = 5$, the overall Nusselt number and Sherwood number are greater than 1.0, which can be maintained at $N \geq 0.1$. For the diffusion-dominated solutions, using the flow patterns of Fig. 2(a) and $N = 0$ as initial distributions, gradually increasing buoyancy ratios from $N = 0$, *Nu* and *Sh* are generally around 1.0, which can be sustained for $N \leq 3.6$. Observing from these figures shown in Figs. 2(b) and 3(b), two huge counter-rotating air circulations of high flow intensities occupy most of the space, which greatly enhances the heat and moisture transport along the strip on the floor. However, observing from figures illustrated in Figs. 2(a) and 3(a), weak multicellular flows presents, which weakens the heat and moisture transfer potentials across this enclosure. These observations also can be illustrated by the heat and moisture transport paths analyzed in aforementioned sections.

CONCLUSION

Double diffusive natural convection in an enclosure with multiple free vents has been numerically investigated. Effects of buoyancy ratios on the flow patterns, heat and mass transfer rates are discussed,

particularly with the multiple flow phenomena.

Contours of streamfunction, heatfunction massfunction can vividly portrait the transport paths of fluid, heat and moisture. Heat and moisture transport potentials can be enhanced or inhibited greatly as appropriate initial distributions were achieved.

REFERENCES

B. Gebhart, Y. Jaluria, R.L. Mahajan, B. Sammakia, (1988), *Buoyancy-Induced Flows and Transport*, Hemisphere Publishing, Bristol, PA, Pp 790-800.

Y.L. Chan, C.L. Tien, (1985a), A numerical study of two-dimensional natural convection in square open cavities, *Numerical Heat Transfer*, 8, 65-80.

Y.L. Chan, C.L. Tien, (1985b), A numerical study of two-dimensional laminar natural convection in shallow open cavities, *Int. J. Heat Mass Transfer*, 28, 603-612.

A.H. Abib, Y. Jaluria, (1988), Numerical simulation of the buoyancy-induced flow in a partially open enclosure, *Numerical Heat Transfer*, 14, 235-254.

D. Angirasa, M.J.B.M. Pourquie, F.T.M. Nieuwstadt, (1992), Numerical study of transient and steady laminar buoyancy-driven flows and heat transfer in a square open cavity, *Numerical Heat Transfer, Part A*, 22, 223-239.

G. Desrayaud, G. Lauriat, (2004), A numerical study of natural convection in partially open enclosures with a conducting side-wall, ASME Journal of Heat Transfer, 126, 76-83.

S.A. Lal, C. Reji, (2009), Numerical prediction of natural convection in vented cavities using restricted domain approach, *Int. J. Heat Mass Transfer*, 52, 724-734.

D.B. Ingham, I. Pop, (2005), *Transport Phenomena in Porous Media*, Elsevier, Oxford.

C. Beghein, F. Haghighat, F. Allard, (1992), Numerical study of double-diffusive natural convection in a square cavity, *Int. J. Heat Mass Transfer*, 35, 833-846.

V.A.F. Costa, (1997), Double diffusive natural convection in a square enclosure with heat and mass diffusive walls, *Int. J. Heat Mass Transfer*, 40, 4061-4071.

A.J. Chamkha, H. Al-Naser, (2002), Hydromagnetic double-diffusive convection in a rectangular enclosure with opposing temperature and concentration gradients, *Int. J. Heat Mass Transfer*, 45, 2465-2483.

F.Y. Zhao, D. Liu, and G.F. Tang, (2007), Application issues of the streamline, heatline and massline for conjugate heat and mass transfer, *Int. J. Heat Mass Transfer*, 50, 320-334.

D. Liu, F.Y. Zhao, G.F. Tang, (2008), Thermosolutal convection in a saturated porous enclosure with concentrated energy and solute sources, *Energy Conversion and Management*, 49, 16-31.

F.Y. Zhao, D. Liu, G.F. Tang, (2008), Natural convection in an enclosure with localized heating and salting from below, *Int. J. Heat Mass Transfer*, 51, 2889-2904.

F.Y. Zhao, G.F. Tang, D. Liu, (2006), Conjugate natural convection in enclosures with external and internal heat sources, *International Journal of Engineering Science*, 44, 148-165.

S.V. Patankar, (1980), *Numerical Heat Transfer and Fluid Flow*, Hemisphere, New York.

T. Hayase, J.A.C. Humphrey, R. Greif, (1992), A consistently formulated QUICK scheme for fast and stable convergence using finite-volume iterative calculation procedure, *Journal of Computational Physics*, 98, 108-118.

F.Y. Zhao, D. Liu, G.F. Tang, (2009), Numerical determination of boundary heat fluxes in an enclosure dynamically with natural convection through Fletcher-Reeves gradient method, *Computers & Fluids*, 38, 797-809.